

Review

# Representative High-Temperature Hydrothermal Activities in the Himalaya Geothermal Belt (HGB): A Review and Future Perspectives

Qing Li <sup>1,2,3</sup>, Yanchun Hao <sup>3</sup>, Chuanxin Liu <sup>1</sup>, Jinhang Huang <sup>4</sup> and Xingcheng Yuan <sup>4,\*</sup> 

<sup>1</sup> Jiangsu Transportation Science and Research Institute Corporation of China, Nanjing 210017, China; ql123456yy@sina.com (Q.L.)

<sup>2</sup> School of Civil Engineering, Southeast University, Nanjing 211112, China

<sup>3</sup> China Railway Construction Kunlun Investment Group Company Limited, Chengdu 610040, China

<sup>4</sup> Faculty of Geosciences and Engineering, Southwest Jiaotong University, Chengdu 611756, China

\* Correspondence: yxcheng0722@163.com; Tel.: +86-18223242939

**Abstract:** Southern Tibet and western Yunnan are areas with an intensive distribution of high-temperature geothermal systems in China, as an important part of the Himalayan Geothermal Belt (HGB). In recent decades, China has conducted systematic research on high-temperature geothermal fields such as Yangbajing, Gudui, and Rehai. However, a comprehensive understanding has not yet been formed. The objective of this study was to enhance comprehension of the high-temperature geothermal system in the HGB and to elucidate the hydrogeochemical characteristics of geothermal fluids. This will facilitate the subsequent sustainable development and exploitation of domestic high-temperature hydrothermal geothermal resources. To this end, this study analysed geothermal spring and borehole data from the Yangbajing, Gudui, and Rehai geothermal fields. Based on previous research results, the source, evolution, and reservoir temperature characteristics of geothermal fluids are compared and summarised. The main high-temperature geothermal water in the geothermal field is derived from the deep Cl-Na geothermal fluid. Yangbajing's and Gudui's geothermal waters are primarily recharged by snow-melt water, while Rehai's geothermal water is mainly recharged by local meteoric water. The average mixing ratios of magmatic water in the Yangbajing, Gudui, and Rehai geothermal fields are 17%, 21%, and 22%, respectively. The Yangbajing and Gudui geothermal fields have a relatively closed geological environment, resulting in a stronger water-rock interaction compared to the Rehai geothermal field. As geothermal water rises, it mixes with shallow cold water infiltration. The mixing ratios of cold water in the Yangbajing, Gudui, and Rehai geothermal fields are 60–70%, 40–50%, and 20–40%, respectively. Based on the solute geothermometer calculations, the maximum geothermal reservoir temperatures for Yangbajing, Gudui, and Rehai are 237 °C, 266 °C, and 282 °C, respectively. This study summarises and compares the hydrogeochemical characteristics of three typical high-temperature geothermal fields. The findings provide an important theoretical basis for the development of high-temperature geothermal resources in the Himalayan Geothermal Belt.

**Keywords:** hydrothermal activity; Himalayan Geothermal Belt; recharge source; geothermal reservoir; hydrochemical process



**Citation:** Li, Q.; Hao, Y.; Liu, C.; Huang, J.; Yuan, X. Representative High-Temperature Hydrothermal Activities in the Himalaya Geothermal Belt (HGB): A Review and Future Perspectives. *Water* **2024**, *16*, 1378. <https://doi.org/10.3390/w16101378>

Academic Editor: Cesar Andrade

Received: 15 March 2024

Revised: 1 May 2024

Accepted: 3 May 2024

Published: 12 May 2024



**Copyright:** © 2024 by the authors. Licensee MDPI, Basel, Switzerland. This article is an open access article distributed under the terms and conditions of the Creative Commons Attribution (CC BY) license (<https://creativecommons.org/licenses/by/4.0/>).

## 1. Introduction

In the 20th century, with the rapid development of society, energy shortages, environmental pollution, and global warming became increasingly serious. Geothermal energy, as a clean and renewable energy source, has attracted attention and development in over 90 countries, including China, the United States, Iceland, and Italy [1–3]. In 2022, the National Energy Administration of China issued a five-year proposal to improve geothermal mining and accelerate the development of new clean energy. The goal is to achieve

carbon neutrality and optimise the national energy layout by 2060 [4]. China has abundant geothermal resources, of which hydrothermal geothermal resources are equivalent to 125,000 billion tons of standard coal [5]. The annual amount of hydrothermal geothermal resources that can be extracted is  $5.5 \times 10^{19}$  J, equivalent to 1.9 billion tons of standard coal. This could theoretically reduce emissions of CO<sub>2</sub> by 4.9 billion tons. The power generation potential of high-temperature geothermal resources in these hydrothermal resources reaches  $7.12 \times 10^6$  kW [5,6]. However, the current exploration and development of high-temperature geothermal resources is limited in scale and utilization. It is necessary to fully develop and utilize high-temperature geothermal resources and actively promote research, exploration, and development in this area.

Geothermal systems can be classified into three types based on the reservoir temperature: low-temperature (<90 °C), medium-temperature (90–150 °C), and high-temperature (>150 °C) [7]. High-temperature geothermal systems have been extensively studied for geothermal energy development in recent decades due to their significant potential for power generation [8–10]. Their locations are tightly controlled by regionally relevant fault groups, and in the central region they generate a large amount of CO<sub>2</sub> emissions through fracture zones [11,12]. The heat source is the most crucial factor in the formation of high-temperature geothermal systems. This typically includes magmatic heat, heat from the decay of radioactive elements such as <sup>238</sup>U and <sup>232</sup>Th, and frictional heat in the overlapping part of the lithosphere [13–16]. Most geothermal systems have geothermal reservoirs located deep underground. Groundwater acts as a heat carrier and, under the action of convection, flows upward to form a hydrothermal system near the surface. This system is usually expressed through geothermal springs, fountains, hot water rivers, vents, sinters, and hydrothermal alteration [17]. Thermal springs are a natural outlet for geothermal water. Studying their hydrochemical and isotopic characteristics can provide a profound understanding of geothermal systems [18–20]. This includes revealing the source, circulation mechanism, and reservoir characteristics of geothermal water [21–23].

The Himalayan Geothermal Belt (HGB) is a highly active region for geothermal activity in China, including the Tibetan geothermal belt, the western Sichuan geothermal belt, and the western Yunnan geothermal belt. The hydrothermal activity is a result of the collision between the Eurasian and Indian plates [24,25]. The fault zone contains over 400 geothermal springs, primarily controlled by faults and fracture zones, which serve as channels for geothermal fluid migration [26]. Furthermore, the spatial distribution of geothermal water aligns with the spatial distribution of Cenozoic magmatic activity [27]. There are several typical magmatic high-temperature geothermal fields in China, including the Yangbajing and Gudui geothermal fields in Tibet, and the Rehai geothermal field in Yunnan [28] (Figure 1). In 1977, the Yangbajing high-temperature geothermal field in Tibet successfully achieved geothermal power generation. By 2014, cumulative power generation had reached 3.11 billion kWh [5,29]. The Gudui geothermal field is rich in geothermal resources. It is the geothermal field with the highest temperature at the same depth in China. It is a typical shallow high-temperature geothermal field. It is the geothermal field with the highest potential discovered in China after Yangbajing [30]. The Tengchong geothermal field is divided into 58 hydrothermal activity areas, including 24 geothermal spring groups with average temperatures over 45 °C and 3 boiling spring groups. The Rehai geothermal field is the most intense geothermal field in Tengchong, and is considered to have great development potential [31].

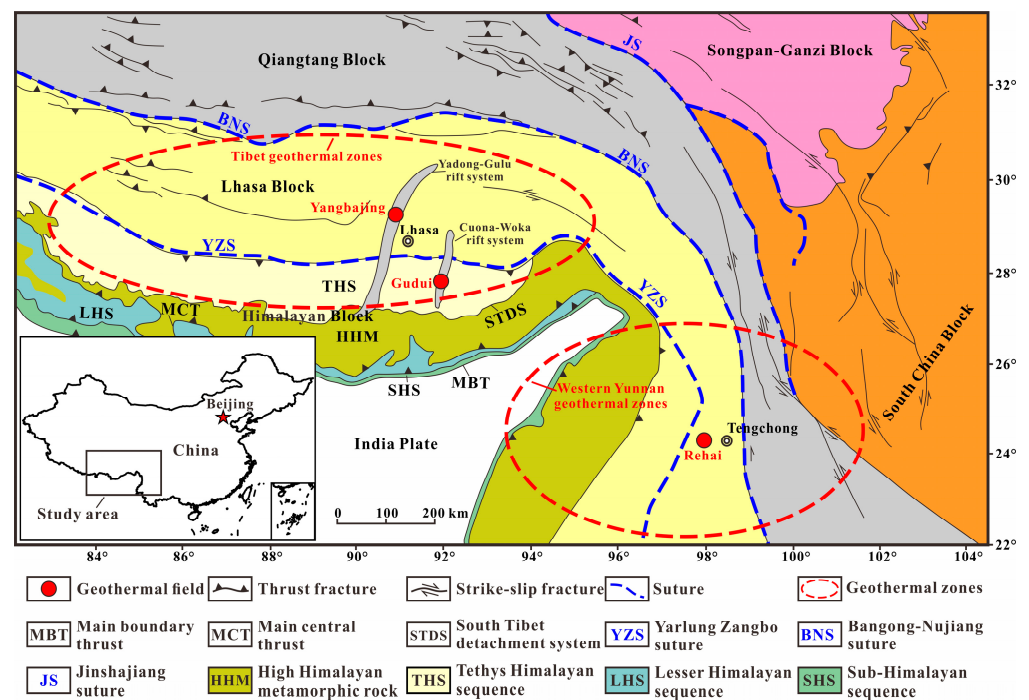


**Figure 1.** Simplified tectonic map of the HGB [32]. The red dots represent the three geothermal fields in this study, and the red dashed circles represent the Tibetan and western Yunnan geothermal zones.

To enhance comprehension of the high-temperature geothermal systems in the Himalayas and facilitate the development and utilization of high-temperature hydrothermal geothermal resources, this paper summarises the existing hydrochemical and isotopic data of geothermal water. The focus is on the similarities and differences in the hydrogeochemical characteristics of the Yangbajing, Gudui, and Rehai geothermal systems.

## 2. Geological and Geothermal Background of the HGB

### 2.1. Regional Geological Structure Settings

The study of tectonic evolution history has revealed that the Tibetan Plateau is the most typical continental collision orogenic belt in the world, formed by the India–Eurasian collision. It has undergone three stages of evolution: main collision convergence (65–41 Ma), late collision transition (40–26 Ma), and post-collision extension (25–0 Ma) [33]. Due to tectonic influence, the Tibetan Plateau is divided into four terranes from north to south, namely, Songpan-Ganzi, Qiangtang, Lhasa, and Himalaya, and the Himalayan terrane consists of the Tethys-Himalayan sequence, the High Himalayan metamorphic rock, the Lesser Himalayan sequence, and the Sub-Himalayan sequence (Figure 1). The terranes are separated by the Jinsha River suture zone, Bangong–Nujiang River suture zone, and Yarlung–Zangbo River suture zone, which trend nearly east to west. Numerous thrust and strike-slip fractures are developed in the east, and the south Tibet detachment system, main central thrust, and main boundary thrust are developed in the south [34,35] (Figure 1). Following the large-scale uplift of the Qinghai–Tibet Plateau during the Miocene period, the E-W extension was reinforced, resulting in a series of nearly N-S-trending fault that intersected the Bangong–Nujiang River suture zone and the Yarlung–Zangbo River suture zone. These fault systems locally developed into a rift or graben basin of a certain scale, which controlled the Miocene volcanic activity in southern Tibet and induced strong modern hydrothermal activity, forming the Himalayan large-scale geothermal belt, including the Tibet geothermal zones and the western Yunnan geothermal zones [36,37]. The Yangbajing and Gudui geothermal fields belong to the Tibet geothermal zones, of which the Yangbajing geothermal field is located in the Yadong–Gulu rift system and the Gudui geothermal field is located in the Cuona–Woka rift system [38]. The Gudui geothermal field is located in the

N-S-trending Cuona–Woka rift zone in the Tethys-Himalayan tectonic belt [39]. The Rehai geothermal field belongs to the western Yunnan geothermal zones, which is located on the eastern side of the collision zone between the Eurasian and Indian plates [40,41].

The Yangbajing geothermal field comprises two groups of NNE-SSW and NE-SW faults (Figure 2a). These faults are all tensile active faults that intersect or cut through each other to form a prismatic structural pattern. It is inferred that these extended faults were active until the late Quaternary as flow channels for geothermal fluid storage and migration [42]. The Gudui geothermal field is characterised by geotectonic activities, with 14 faults oriented in near-E-W and -N-S directions (Figure 2b). The E-W-trending faults in the area were formed in the early stage of tectonic activity, and most of them were reverse faults. The rock in the fault fracture zone is dense and exhibits poor permeability due to the influence of compressive stress. The N-E- and N-W-trending faults were formed during the late tectonic period, creating a pathway for geothermal fluid to ascend [43]. The Gudui geothermal springs are situated at the intersection of faults and their vicinity, suggesting that the formation of the Gudui geothermal field is influenced by tectonic activity. Previous studies analysed and studied the He isotope composition of the gas that escaped from the springs in the Rehai geothermal field [44,45]. The results indicate that the release of modern mantle-derived He in the Rehai area is primarily controlled by multiple sets of active faults at varying depths. The near-N-S-trending faults, which are distributed along the Laogunguo, Dagunguo, Xiaogunguo, and Huangguaqing lines, cut the crust the deepest. The N-W-trending faults follow, and the N-E-trending faults, that may control the springs on the south bank of the Zaochang River, are the shallowest (Figure 2c). These three sets of faults in the geothermal field are the main channels for geothermal fluid migration [45,46].

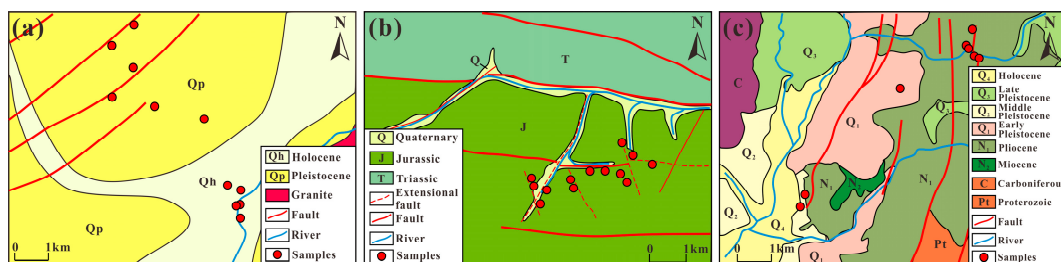


**Figure 2.** Local simplified geological maps of Yangbajing (a) [19], Gudui (b) [43], and Rehai (c) [47]. The red circles in the figure represent the locations of some of the geothermal water samples.

The magmatic rocks exposed around the Yangbajing geothermal field consist mainly of late Yanshan Himalayan granites, with a K-Ar radiation age of 8.1 Ma. But so far, no Quaternary volcanic activity has been discovered in the Yangbajing area. The INDEPTH (International Deep Profiling of Tibet and the Himalayas) project has identified “bright spots” that suggest the heat source of the geothermal system is a partial melting body located at a depth of 15–20 km [38,48]. The existence of the Yangbajing magmatic heat source was confirmed in a series of articles [49–51]. Therefore, it can be inferred that the magmatic heat source is responsible for the formation of high-temperature geothermal fluid in the Yangbajing geothermal field. Magmatic intrusion activities occur frequently in the Gudui geothermal field, but the scale of intrusion is small. The intrusions consist mainly of Early Cretaceous diorite and Late Cretaceous diabase [43]. Magnetotelluric sounding has discovered a large low-resistivity zone located 15–30 km beneath the study area, which is thought to be localized melt bodies. This zone acts as the main heat source driving the regional geothermal activity [30,52]. Tengchong is a well-known geothermal area with an extensive distribution of volcanic rocks. The volcanic outcrops, which include basalts, andesitic basalts, andesites, and diorites, cover an area of over 1000 km<sup>2</sup>. Additionally, there are older granite, diorite granite, syenite, and quartz porphyry in the Tengchong area [46]. The Rehai geothermal field’s basement is composed of Yanshanian granite, which only outcrops in a few small areas and its age is 68.8 million years [31]. At a depth of 7 km below the Rehai geothermal field, there is a magma chamber that retains water and has a

thickness of 20 km. This magma chamber serves as a heat source and significantly impacts the formation of high-temperature geothermal fluid in the Rehai geothermal system [53].

## 2.2. Hydrothermal Characteristics of the HGB

The geothermal springs in Tibet, western Yunnan, and western Sichuan are distributed in a belt-like manner. They are located on the collision orogenic belt between the Eurasian plate and the Indian plate and have the same tectonic origin. The geothermal springs are mainly distributed in Tibet and western Yunnan. These areas are collectively called the Yunnan–Tibet geothermal zone [54].

The Yunnan–Tibet geothermal belt is a significant part of the HGB. Since the Cenozoic era, a convergent continental margin active zone has formed in Tibet and western Yunnan due to the collision between the Indian plate and the Eurasian plate. These areas exhibit the strongest tectonic activity and are accompanied by robust hydrothermal activity, creating favourable conditions for the formation of high-temperature hydrothermal systems [55]. The Yangbajing geothermal field, Gudui geothermal field in southern Tibet, and Rehai geothermal field in western Yunnan exhibit strong hydrothermal activity and high-temperature geothermal manifestations. These areas have long been favoured by geoscientists and have yielded rich research results [42,43,46].

The activity of geothermal water in Tibet is influenced by plate tectonics and active tectonics. There are over 600 hydrothermal manifestation areas, mostly located near the plate and active tectonic belt, forming the corresponding geothermal active belt [56]. The Yangbajing geothermal field is a non-volcanic high-temperature geothermal field located in the Dangxiong–Yangbajing fault basin at the southeastern foot of the Nyainqentanglha Mountains in the HGB. The basin experiences strong neotectonic activity, which has led to the development of fault structures and increased hydrothermal activity. The surface exhibits various hydrothermal activities, including boiling springs, vents, hot water marshes, lakes, ponds, and sinter deposits. The Yangbajing geothermal system comprises two distinct geothermal reservoirs: a shallow one, with a depth of 180–280 m; and a deep one, with a depth of 950–1850 m [57]. Based on the logging records of borehole ZK4002, the temperature of the shallow reservoir ranges from 130 °C to 173 °C, while the deep reservoir temperature ranges from 240 °C to 329.8 °C [42]. The Gudui geothermal field is situated in the Cuona–Woka rift zone, which runs north–south in the Tethys-Himalayan tectonic belt. It is a non-volcanic geothermal system with a variety of surface hydrothermal activity types, including geothermal springs, boiling springs, fountains, travertine, silicic, and surrounding rock alteration [39]. The Geothermal Brigade of Tibet Geological Bureau drilled three boreholes, namely, ZK251, ZK301, and ZK302, in the Gudui geothermal area. Geothermal fluids were produced at temperatures of 163 °C, 159 °C, and 205 °C, respectively. The temperature of the ZK302 geothermal borehole reached 205 °C at a depth of 230 m, setting a new record for the highest temperature at that depth in geothermal exploration in China [43]. The Rehai geothermal field is located in the north-central part of the Tengchong–Longchuan hydrothermal activity zone and is located at the top of the outer arc of the Guyong–Dayingjiang arc fault. It is a large-scale geothermal field with a wide range of hydrothermal activities, high intensity, and all types of hydrothermal activities in the Tengchong area. This field is a typical high-temperature geothermal field of the volcanic type. Hydrothermal activities include hydrothermal explosions, geysers, jet holes, and boiling springs [55]. The Tengchong volcanic area contains three magma chambers, one of which is situated beneath the Tengchong–Heshun–Rehai geothermal field. This particular chamber, located at a depth of approximately 6–7 km, has a current temperature range of 438 °C to 773 °C and serves as the primary heat source for the Rehai geothermal field. It plays an important role in the formation of the geothermal system [58].

### 3. Material and Methods

#### 3.1. Data Collection

To systematically understand the formation of high-temperature hydrothermal activities in the Yunnan–Tibet geothermal belt, this paper analyses 258 groups of geothermal water physical and chemical data. The data were collected from published papers in recent years and from the three geothermal fields of Yangbajing, Gudui, and Rehai, as reported in “Geothermal Resources in China” [59]. The analysis includes 174 groups of hydrochemical data (Table S1) and 84 groups of stable hydrogen and oxygen isotope data (Table S2). The data selection criteria were as follows: (1) Geothermal water samples should have complete or convertible measurements of  $\text{Na}^+$ ,  $\text{K}^+$ ,  $\text{Ca}^{2+}$ ,  $\text{Mg}^{2+}$ ,  $\text{SO}_4^{2-}$ ,  $\text{HCO}_3^-$ ,  $\text{Cl}^-$ , and  $\text{SiO}_2$ . Additionally, a spring temperature should be recorded concurrently with the hydrochemical sampling. (2) The isotope samples data utilise only hydrogen and oxygen stable isotopes, with the sampling elevation also recorded.

#### 3.2. Geochemical Calculations

Stable hydrogen and oxygen isotopes ( $\delta\text{D}$  and  $\delta^{18}\text{O}$ ) were utilized to determine the recharge sources of the geothermal springs. By leveraging the altitude effect associated with  $\delta\text{D}$ , the recharge elevation for the geothermal springs was estimated [2,60] (Equation (1)).

$$H = (\delta R - \delta P) / K + h \quad (1)$$

where  $H(\text{m})$  is the recharge elevation,  $\delta R(\text{‰})$  is the  $\delta\text{D}$  value of the geothermal spring sample,  $\delta P(\text{‰})$  is the  $\delta\text{D}$  value of the shallow groundwater sample,  $K(\text{‰}/100 \text{ m})$  is the isotopic elevation gradient of the atmospheric precipitation, and  $h(\text{m})$  is the elevation of the shallow groundwater sample. The contribution of different recharge waters was also estimated using a mixing model [19,61] (Equations (2)–(5)).

$$\delta K(a) = \delta K(c) \times f(c) + \delta K(d) \times f(d) \quad (2)$$

$$f(c) + f(d) = 1 \quad (3)$$

$$\delta K(a) = \delta K(b) \times f(b) + \delta K(d) \times f(d) \quad (4)$$

$$f(b) + f(d) = 1 \quad (5)$$

where  $\delta K(\text{‰})$  represents the value of  $\delta\text{D}$  or  $\delta^{18}\text{O}$ ; a, b, c, and d denote geothermal spring samples, meteoric water, snow-melt water, and magmatic water, respectively; and  $f(\%)$  represents the contribution of different sources.

When exploring geothermal resources, the temperature of deep geothermal reservoirs is a crucial indicator for distinguishing between types of geothermal systems and evaluating the potential of geothermal resources. However, direct measurement of this parameter is often challenging. A geochemical thermometer can effectively and conveniently obtain this parameter. This paper employs the use of  $\text{SiO}_2$  geothermometers to estimate the temperature of geothermal reservoirs. The empirical formula of the  $\text{SiO}_2$  geothermometer is established through the functional relationship between the solubility of quartz and chalcedony and temperature. When utilising the  $\text{SiO}_2$  geothermometer to calculate temperature, it is necessary to consider the specific geological background of the Yangbajing and Gudui geothermal fields, which are situated at high altitudes. At a sampling temperature of  $80 \text{ }^\circ\text{C}$ , it can be assumed that the boiling point temperature has been reached [62]. The average altitude of the Rehai geothermal field is relatively low, with a boiling point temperature of  $96 \text{ }^\circ\text{C}$  [46]. Consequently, when the sampling temperature reaches the local boiling point, the maximum steam loss of  $\text{SiO}_2$  geothermometers is selected for calculation of the geothermal reservoir temperature. As quartz geothermometers are suitable for high-temperature reservoirs with temperatures above  $150 \text{ }^\circ\text{C}$  (Equations (6) and (7)), and chalcedony geothermometers are suitable for reservoirs

with geothermal water below 180 °C (Equations (8) and (9)), in this study, the results of quartz geothermometers are employed when the reservoir temperature exceeds 150 °C, while those of chalcedony geothermometers are utilised when the reservoir temperature is below 150 °C. The geothermal water is affected by the mixing of shallow cold water during ascent, which reduces the SiO<sub>2</sub> content. This results in the calculation of a smaller value from the SiO<sub>2</sub> geothermal meters, which can be regarded as the average temperature of the geothermal field or the lower limit of the temperature of the geothermal reservoir [30].

$$T_{\text{quartz1}} = \frac{1309}{5.19 - \log(\text{SiO}_2)} - 273.15 (\text{No steam loss}) \quad (6)$$

$$T_{\text{quartz2}} = \frac{1522}{5.75 - \log(\text{SiO}_2)} - 273.15 (\text{Maximum steam loss}) \quad (7)$$

$$T_{\text{chalcedony1}} = \frac{1032}{4.69 - \log(\text{SiO}_2)} - 273.15 (\text{No steam loss}) \quad (8)$$

$$T_{\text{chalcedony2}} = \frac{1264}{5.31 - \log(\text{SiO}_2)} - 273.15 (\text{Maximum steam loss}) \quad (9)$$

#### 4. Genesis of Representative High-Temperature Hydrothermal Activities in the HGB

##### 4.1. Hydrogeochemical Evolution Process of Yangbajing Geothermal Field

##### 4.1.1. Hydrochemical Type

The main cation in Yangbajing geothermal water is Na<sup>+</sup> and the predominant anion is Cl<sup>-</sup>, followed by HCO<sub>3</sub><sup>-</sup>. The contents of Mg<sup>2+</sup>, Ca<sup>2+</sup>, K<sup>+</sup>, and SO<sub>4</sub><sup>2-</sup> in the geothermal water is relatively low (Figure 3). The geothermal spring water exposed in the Yangbajing geothermal field was mainly of the Cl-Na type, with some also being of the Cl·HCO<sub>3</sub>-Na type (Figure 4). The hydrochemical type of the shallow groundwater was HCO<sub>3</sub>-Ca (Figure 4). The chemical characteristics of the geothermal water and shallow groundwater differed significantly. The hydrochemical type may be related to the reservoir lithology of the geothermal field, which is rich in silicate minerals such as granite and sandstone [17]. Interestingly, the mixing process of geothermal water and cold water was also observed: Cl-Na type geothermal water (deep reservoir) mixed with HCO<sub>3</sub>-Ca·Na type water (cold groundwater) to form Cl·HCO<sub>3</sub>·Na and HCO<sub>3</sub>-Cl·Na type geothermal water (shallow reservoir) [63] (Figure 4). The shallow reservoir in Yangbajing is formed by the upward flow of geothermal fluid from the deep reservoir into the Quaternary aquifer, which is the source of the cold groundwater [42].

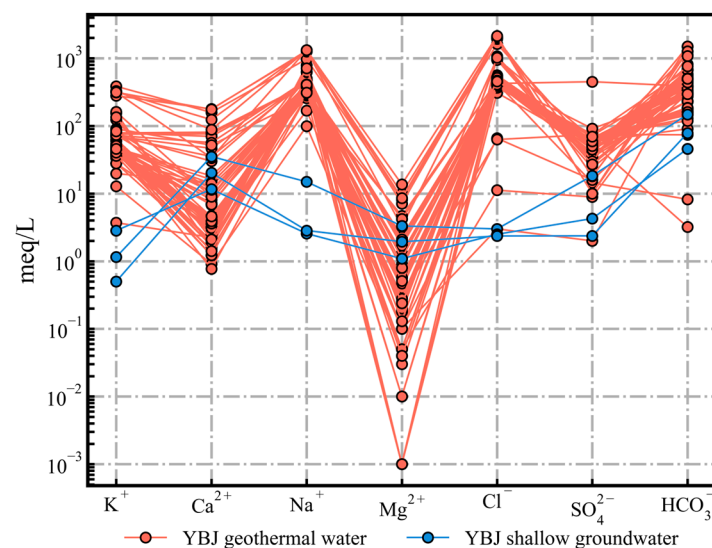


Figure 3. The Schoeller diagram of Yangbajing geothermal water.

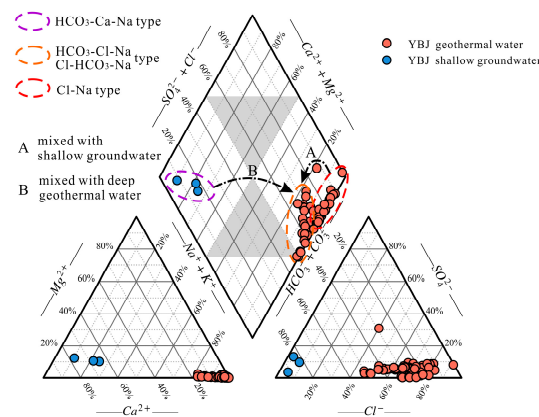


Figure 4. Piper trilinear diagram [64] of the Yangbajing geothermal water.

#### 4.1.2. Recharge Source of Geothermal Water

The  $\delta D$  values in the Yangbajing geothermal field ranged from  $-158.15\text{‰}$  to  $-139.6\text{‰}$ , while the  $\delta^{18}O$  values varied from  $-20.4\text{‰}$  to  $-16.6\text{‰}$  (Table S2). Based on previous research results, the global meteoric water line (GMWL:  $\delta D = 8\delta^{18}O + 10$ ) [65] and the local meteoric water line (LMWL:  $\delta D = 8.01\delta^{18}O + 11.8$ ) [56] were drawn. The sources of recharge for geothermal water in Yangbajing may consist of three end-members: magmatic water (rectangle A) [60], meteoric water (rectangle B) [8], and snow-melt water (rectangle C) [19]. The shallow groundwater in Yangbajing is situated on the LMWL and is closed to the meteoric water end, indicating the shallow groundwater mainly comes from atmospheric precipitation (Figure 5). The points of geothermal water deviate from the meteoric water line and are distributed along a straight line connecting the magmatic water end and the snow-melt water end. This suggests that the primary sources of geothermal water in Yangbajing are the local snow-melt water and magmatic water [38,60]. The binary isotope mixing model (Equations (2) and (3)) estimates that the mixing ratio of magmatic water in Yangbajing geothermal water is between 10% and 22% (Table S2). The recharge elevation of geothermal water in Yangbajing has been calculated, using the elevation gradient of  $\delta D$  in the eastern Qinghai–Tibet Plateau ( $-2.6\text{‰}/100\text{ m}$ ) [66], to be between 5174 m and 5736 m (Equation (1), Table S2). This elevation range is located near the footwall of the slip fault system on the southern margin of Nianqingtanglha. It is consistent with the distribution elevation of the local snow line and the source of the shallow groundwater system [42]. Therefore, the geothermal water in this area originates from snow meltwater from the Nyainqentanglha Mountains that infiltrates into the underground through deep circulation along the fault zone and is heated and convected by the deep magmatic heat source [57].

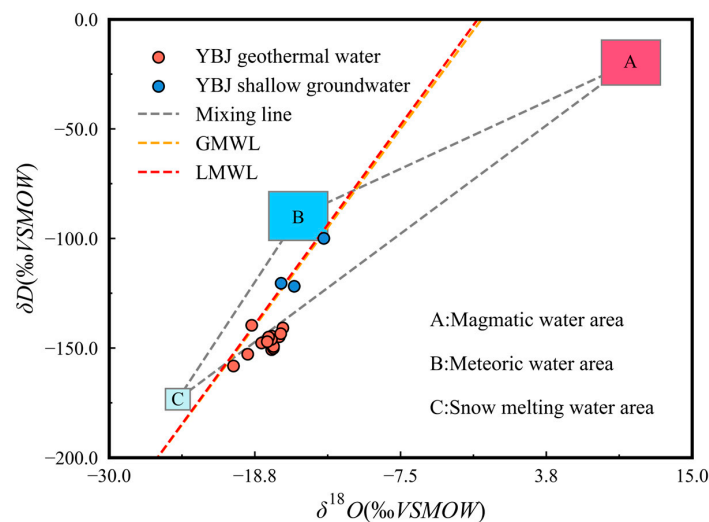
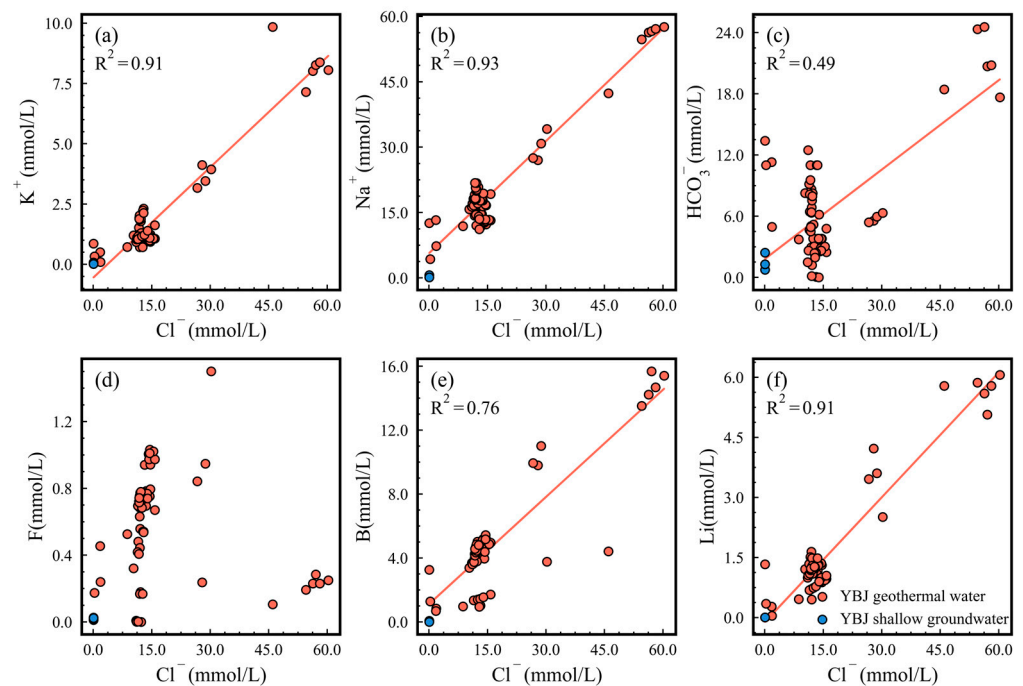


Figure 5. The relationship between  $\delta D$  and  $\delta^{18}O$  values of Yangbajing geothermal water.

#### 4.1.3. Effects of Deep Geothermal Fluid

The  $\text{Na}^+$ ,  $\text{K}^+$ , and other components in the geothermal water are derived primarily from the leaching of the surrounding rock. While the water–rock interaction in the geothermal reservoir contributes to the  $\text{Cl}^-$  content, this contribution to the high-temperature hydrothermal system with a magmatic heat source is significantly less than that of  $\text{Cl}^-$  obtained from the degassing process of the magma [67,68]. A significant positive correlation has been identified between the concentrations of  $\text{Na}^+$ ,  $\text{K}^+$ , and  $\text{Cl}^-$  in the Yangbajing geothermal field (Figure 6). This suggests that the geothermal water originates from a similar deep geothermal reservoir [31,46].  $\text{B}$  and  $\text{Cl}^-$  in geothermal water are primarily derived from deep materials, and water–rock interaction has a minimal impact on them. They do not precipitate from the solution during migration [63]. The concentrations of  $\text{B}$  and  $\text{Cl}^-$  in deep and shallow geothermal water vary considerably, yet maintain a strong linear relationship. This suggests that the deep and shallow geothermal waters in the Yangbajing geothermal field share a common geothermal origin. The  $\text{Na}^+$ ,  $\text{K}^+$ ,  $\text{B}$ ,  $\text{Li}$ , and other components in the geothermal water exhibit aggregation characteristics in the area, with  $\text{Cl}^-$  contents of 13 mmol/L and 63 mmol/L. This is due to the existence of deep and shallow binary geothermal reservoirs. The geothermal water samples exhibit a high component content in the geothermal water derived from the deep geothermal reservoir. These components display an evident linear distribution trend, indicating that the geothermal water is subject to mixing during the rising process [69].



**Figure 6.** Correlation diagram of  $\text{Cl}^-$  and other hydration components of Yangbajing geothermal water. (a)  $\text{K}^+$  vs.  $\text{Cl}^-$  (b)  $\text{Na}^+$  vs.  $\text{Cl}^-$  (c)  $\text{HCO}_3^-$  vs.  $\text{Cl}^-$  (d)  $\text{F}$  vs.  $\text{Cl}^-$  (e)  $\text{B}$  vs.  $\text{Cl}^-$  (f)  $\text{Li}$  vs.  $\text{Cl}^-$ .

#### 4.1.4. Analysis of Water–Rock Equilibrium State

In the  $\text{Na}$ – $\text{K}$ – $\text{Mg}$  diagram, most of the Yangbajing geothermal water samples are partially equilibrated waters (Figure 7). This suggests that the geothermal water is in a state of partial equilibrium with albite and potassium feldspar in the subsurface [13]. The geothermal water is distributed primarily along the  $\text{Na}$ – $\text{K}$  isotherm of 240 °C, indicating the mixing of hot and cold end-members and revealing the characteristics of the reservoir temperature in magmatic geothermal systems [19]. The Yangbajing geothermal field's reservoir temperature may be around 240 °C. As the majority of the Yangbajing geothermal water does not belong to fully equilibrated waters, there will be a significant difference

between the estimated geothermal reservoir temperature and the actual situation when applying the cationic geothermometers (Na-K and K-Mg geothermometers, etc.).

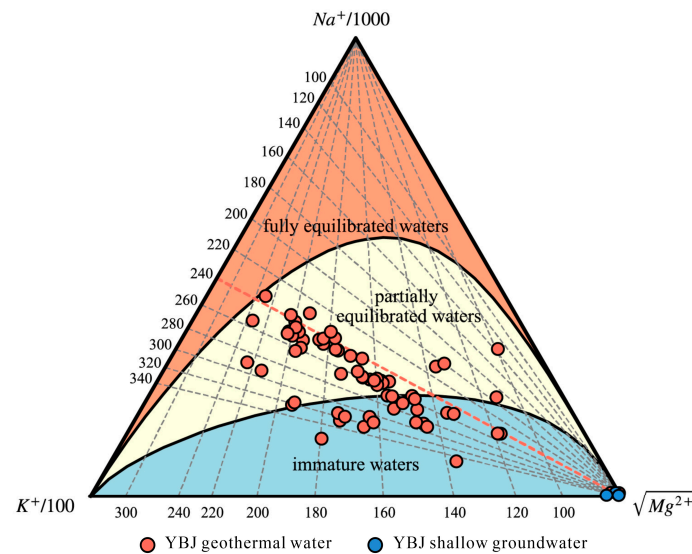


**Figure 7.** The Na–K–Mg triangle diagram [70] of Yangbajing geothermal water.

#### 4.1.5. Reservoir Temperature

The quartz geothermometers estimate that the thermal reservoir temperature of Yangbajing is between 110 °C and 237 °C, with an average of 165 °C. The temperature of the Yangbajing geothermal reservoir is estimated to be between 84 °C and 223 °C by chalcedony geothermometers, with an average of 143 °C (Table S1). Given that the estimated mean values of the two methods are both below 180 °C, the estimated mean value (143 °C) of the chalcedony geothermometers was employed as the shallow geothermal reservoir temperature of Yangbajing. In accordance with the findings of previous research, the maximum temperature (237 °C) estimated by the quartz geothermometer represents the temperature of the deep geothermal reservoir in Yangbajing [38,57].

## 4.2. Hydrogeochemical Evolution Process of Gudui Geothermal Field

### 4.2.1. Hydrochemical Type

The primary cation of the Gudui geothermal system is  $\text{Na}^+$ , while its primary anions are  $\text{Cl}^-$  and  $\text{HCO}_3^-$  (Figure 8). The concentrations of  $\text{Ca}^{2+}$  and  $\text{Mg}^{2+}$  are minimal, whereas the ion characteristics of the shallow groundwater and cold springs are opposite. The concentrations of  $\text{Ca}^{2+}$ ,  $\text{Mg}^{2+}$ , and  $\text{SO}_4^{2-}$  are higher than in most geothermal waters. The hydrochemical type of geothermal water in the Gudui is mainly the Cl-Na type, in addition to Cl· $\text{HCO}_3$ -Na. The hydrochemical type of the local shallow groundwater is the  $\text{SO}_4$ · $\text{HCO}_3$ -Ca·Mg type (Figure 9). The hydrochemical characteristics of the geothermal water and shallow groundwater are obviously different. The surface cold water's characteristics may be attributed to the absorption of steam and gas from the deep hydrothermal system by the surface groundwater. This water may remain above the low-permeability cap rock, resulting in the formation of water rich in  $\text{SO}_4^{2-}$  [71]. The presence of a strong sulphur smell in geothermal water may indicate a high concentration of  $\text{H}_2\text{S}$  in the flash gas. Since Cl does not typically migrate with flash vapour, the concentration of Cl in shallow groundwater and cold springs is low [43]. In the shallow underground environment,  $\text{H}_2\text{S}$  dissolved in groundwater is oxidized to  $\text{SO}_4^{2-}$ . This process results in the acidification of cold springs and shallow groundwater, making them rich in  $\text{SO}_4^{2-}$ . Exposed surface geothermal water is closely related to deep thermal fluid, and this type of water is often rich in  $\text{CO}_2$  and  $\text{H}_2\text{S}$ . Geothermal fluids may be affected by the mixing of near-surface cold water, eventually forming Cl· $\text{HCO}_3$ -Na type water (Figure 9). With increased intensity of action, it may also transition to  $\text{HCO}_3$ ·Cl-Na type water [30].

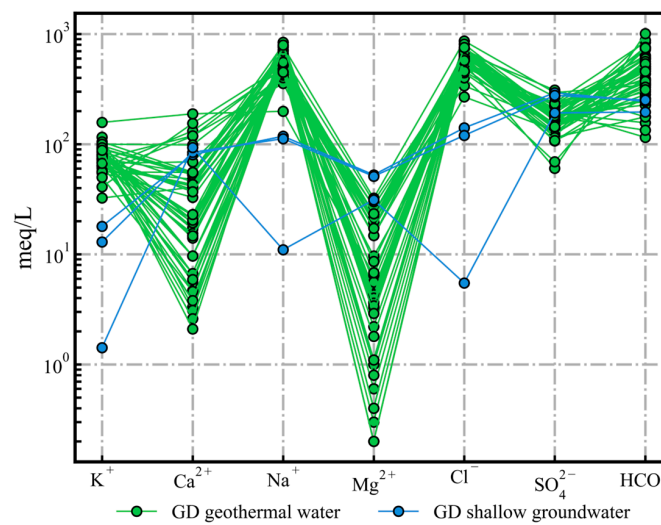


Figure 8. The Schoeller diagram of Gudui geothermal water.

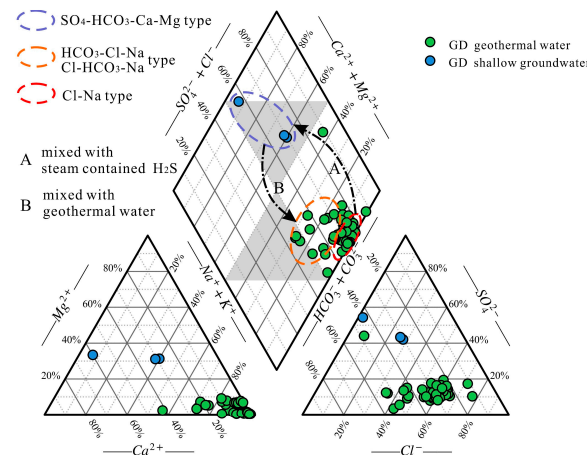


Figure 9. Piper trilinear diagram [64] of the Gudui geothermal water.

#### 4.2.2. Recharge Source of Geothermal Water

The  $\delta D$  values in the Gudui geothermal field range from  $-147.0\text{‰}$  to  $-129.1\text{‰}$ , while the  $\delta^{18}O$  values range from  $-18.1\text{‰}$  to  $-15.29\text{‰}$  (Table S2). The scatter points of hydrogen and oxygen isotopes in geothermal water and shallow groundwater samples in the study area are generally distributed below the global meteoric water line (GMWL) [65] and the local meteoric water line (LMWL) [34] (Figure 10). The distribution of shallow groundwater scatter points is nearly parallel to the meteoric water line. This is because of the influence of evaporation during rainfall, which causes shallow groundwater isotope data to deviate from the meteoric water line [30]. The geothermal water exhibits a certain degree of “ $^{18}O$  drift”, indicating that water–rock interaction affects the geothermal water during migration. Previous research indicates that the recharge sources of geothermal water in Gudui may consist of three end-elements: magmatic water (rectangle A) [60], meteoric water (rectangle B) [8], and snow-melt water (rectangle C) [19]. The isotope points in the area lie on the straight line that connects magmatic water and snow-melt water. They are located near the end-element of snow-melt water, indicating that the primary sources of geothermal water are local snow-melt water and magmatic water. The mixing ratio of magmatic water in Gudui geothermal water is estimated to be between 17% and 29% (Table S2) by the binary isotope mixing model (Equations (2) and (3)). The recharge elevation of the Gudui geothermal water was estimated to be between 4764 m and 5186 m, utilizing the  $\delta D$  elevation gradient ( $-2.6\text{‰}/100\text{ m}$ ) in the eastern Qinghai–Tibet Plateau, as reported by Yu, Zhang, Yu, and Liu [66] (Equation (1), Table S2). Snow

and ice accumulation persists above 5500 m on the Qinghai–Tibet Plateau throughout the year [34,72]. The recharge elevation of the Gudui geothermal water is near the local snow line.

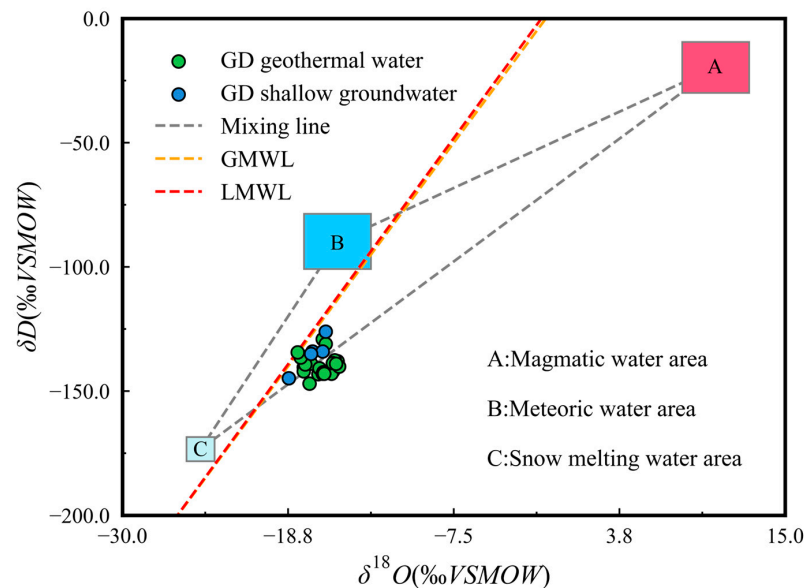


Figure 10. The relationship between  $\delta D$  and  $\delta^{18}O$  values of Gudui geothermal water.

#### 4.2.3. Effects of Deep Geothermal Fluid

There is a certain linear relationship between the Na, K, and Cl in the geothermal water, but the correlation is poor, suggesting that other geochemical behaviours, such as water–rock interaction and ion exchange, greatly affect the geothermal water in the area [73] (Figure 11). The minor element components of geothermal water in the study area are significant (B, F, Li), obtaining the content of this scale from rock leaching is difficult, especially in areas that have experienced long-term hydrothermal activity. Thus, geothermal water in the area is mixed with deep geothermal fluid [30]. The concentrations and ratios of B, F, and Li vary significantly due to variations in underground temperatures and parent rock types in different hydrothermal areas of Gudui. These variations are influenced by different types and degrees of water–rock interaction [43].

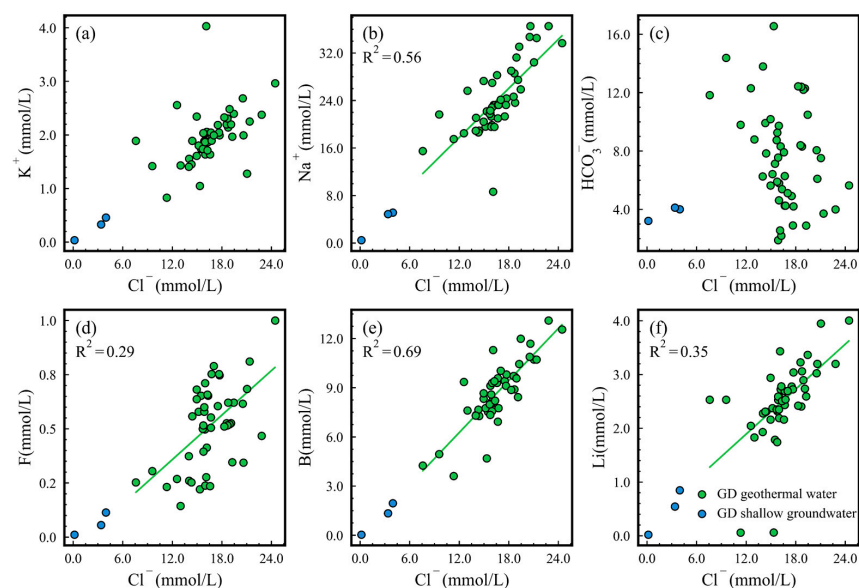
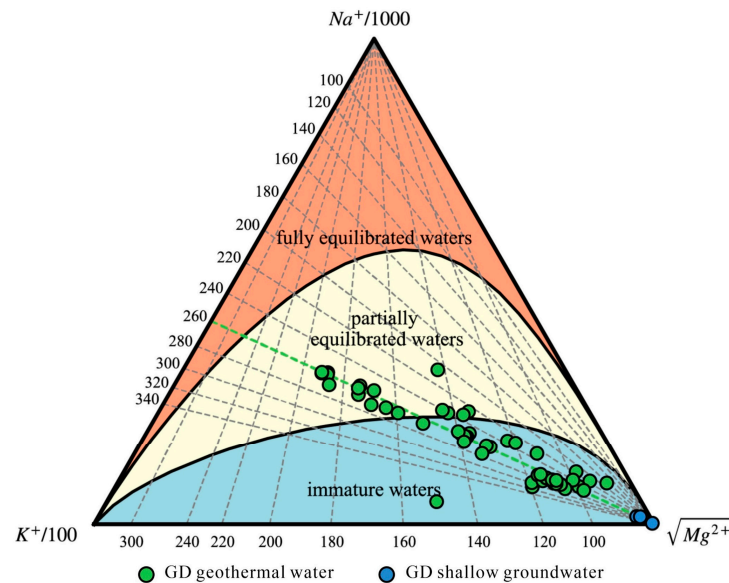


Figure 11. Correlation diagram of  $Cl^-$  and other hydration components of Gudui geothermal water. (a)  $K^+$  vs.  $Cl^-$  (b)  $Na^+$  vs.  $Cl^-$  (c)  $HCO_3^-$  vs.  $Cl^-$  (d) F vs.  $Cl^-$  (e) B vs.  $Cl^-$  (f) Li vs.  $Cl^-$ .

#### 4.2.4. Analysis of Water–Rock Equilibrium State

The majority of the geothermal water in the Gudui geothermal field is classified as immature water (Figure 12). The Na–K–Mg diagram indicates that the Gudui geothermal water follows a distribution trend along the 240 °C Na–K isotherm. This indicates that the geothermal water in Gudui originates from the same parent geothermal fluid, and the temperature of the deep geothermal reservoir can reach 260 °C. During the exposure of geothermal water, it is mixed with shallow cold water to varying degrees [30]. It is inadvisable to employ a cationic geothermometer in estimating the temperature of Gudui geothermal reservoir, as the geothermal water has not yet reached a state of full equilibrium.



**Figure 12.** The Na–K–Mg triangle diagram [70] of Gudui geothermal water.

#### 4.2.5. Reservoir Temperature

The quartz geothermometers estimate that the thermal reservoir temperature of Gudui is between 78 °C and 223 °C, with an average of 159 °C. The temperature of the Gudui geothermal reservoir is estimated to be between 51 °C and 209 °C by chalcedony geothermometers, with an average of 136 °C (Table S1). Given that the estimated mean values of the two methods are both below 180 °C, the estimated mean value (136 °C) of the chalcedony geothermometers was employed as the shallow geothermal reservoir temperature of Gudui. According to the calculation results of Wang and Zheng [43], the temperature of the deep geothermal reservoir in the Gudui geothermal field can reach 266 °C. Therefore, the estimated temperatures of the quartz and chalcedony geothermometers are low. Considering that the geothermal water may be affected by the mixing of cold water during ascent, the estimation results of the SiO<sub>2</sub> geothermometer are low. In this study, 136–266 °C is used to represent the Gudui geothermal reservoir temperature.

### 4.3. Hydrogeochemical Evolution Process of Rehai Geothermal Field

#### 4.3.1. Hydrochemistry Type

The primary ions present in the Rehai geothermal fluids are HCO<sub>3</sub><sup>−</sup> and Na<sup>+</sup> (Figure 13). The Rehai geothermal springs are mainly of the HCO<sub>3</sub>·Cl–Na type, with some of SO<sub>4</sub>·Cl–Na type, HCO<sub>3</sub>·Na·Ca type, and HCO<sub>3</sub>–Ca type (Figure 14). The local shallow groundwater is of the HCO<sub>3</sub>–Ca type. Rehai geothermal water is formed within a volcanic geothermal system. During the rising process, the Cl-rich geothermal water undergoes a gas–liquid phase separation. The gas mainly consists of CO<sub>2</sub>. As geothermal water rises, the temperature and pressure changes enhance the activity of CO<sub>2</sub>, leading to a reaction with the surrounding rock and an increase in the HCO<sub>3</sub><sup>−</sup> and Na<sup>+</sup> contents of the geothermal water [46,74]. The HCO<sub>3</sub>–Ca and HCO<sub>3</sub>–Na geothermal water found in the Rehai geothermal field is formed

due to the deep geothermal fluid rising to the surface and mixing with a large amount of shallow cold water, or being heated solely by rock conduction (Figure 14) [54].

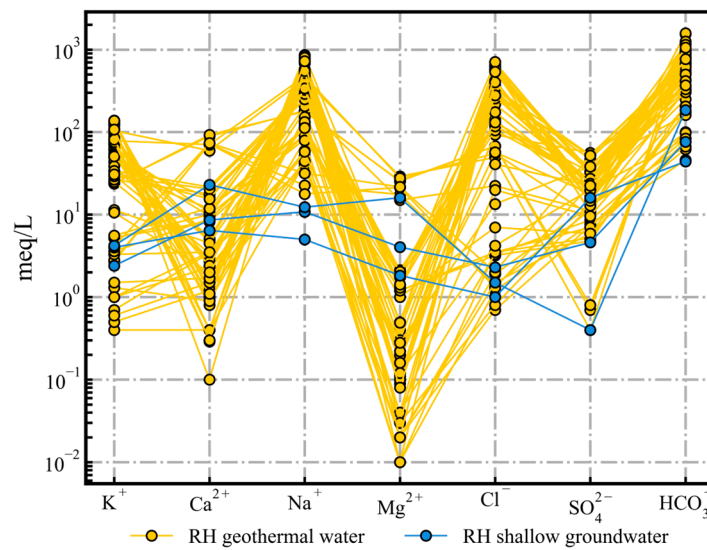


Figure 13. The Schoeller diagram of Rehai's geothermal water.

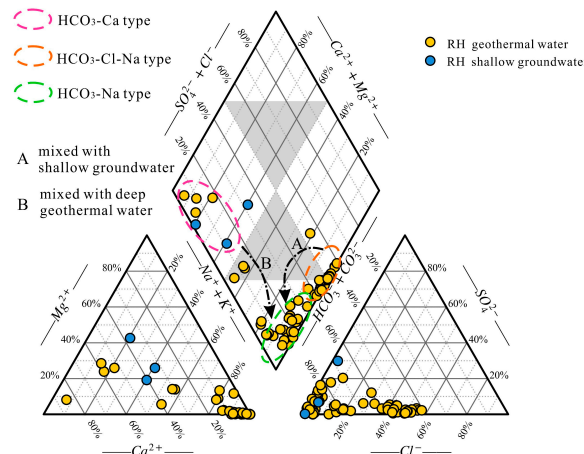
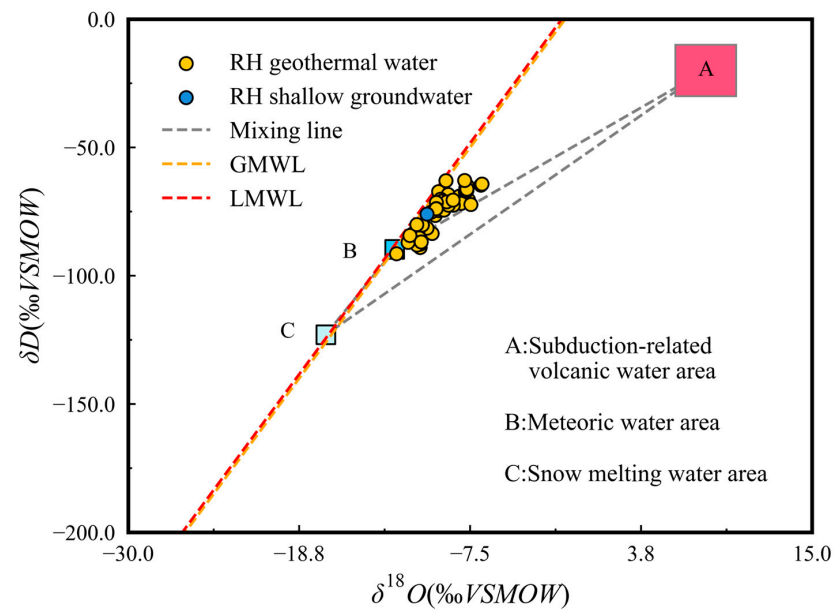


Figure 14. Piper trilinear diagram [64] of the Rehai geothermal water.

#### 4.3.2. Recharge Source of Geothermal Water

The  $\delta D$  values in the Rehai geothermal field range from  $-91.4\text{‰}$  to  $-51.5\text{‰}$ , while the  $\delta^{18}O$  values range from  $-12.35\text{‰}$  to  $-0.47\text{‰}$  (Table S2). The recharge end-member in Rehai comprises subduction-related volcanic water (rectangular A) [40], meteoric water (rectangular B) [40], and snow-melt water (rectangular C) [75]. The hydrogen and oxygen isotope points of geothermal water and shallow groundwater samples in the study area were derived from the meteoric water area and distributed along the GMWL [65] and LMWL [34]. At the same time, some geothermal waters are significantly shifted to the subduction-related volcanic water area (Figure 15). The analysis indicates that geothermal springs primarily receive recharge from meteoric water and are mixed with subduction-related volcanic water during migration. The estimated mixing ratio of subduction-related volcanic water in Rehai's geothermal water ranges from 2% to 37% (Table S2), as determined by the isotope bivariate mixing model (Equations (4) and (5)). The recharge elevation of Rehai's geothermal water was calculated between 1182 m and 2350 m by the elevation gradient of  $\delta D$  ( $-3.0\text{‰}/100\text{ m}$ ) in the eastern Qinghai–Tibet Plateau [76] (Equation (1), Table S2). Combined with the direction of groundwater flow in the Rehai area, it is speculated that the recharge area of the Rehai geothermal springs may be located in the metamorphic rock area of the Gaoligongshan group in the northeastern mountainous area [76].



**Figure 15.** The relationship between  $\delta D$  and  $\delta^{18}O$  values of Rehai’s geothermal water.

### 4.3.3. Effects of Deep Geothermal Fluid

The geothermal water in the area shows a strong linear relationship between  $K^+$ ,  $Na^+$ , and  $Cl^-$ , suggesting the presence of a common parent geothermal fluid [31,46] (Figure 16). There is no linear relationship between the  $Cl^-$  and  $HCO_3^-$  levels. The solubility of thermal-liquid-altered minerals may control these levels [46]. Enrichment of B is typically linked to granite dissolution and magmatic activity, while Li and F are commonly used as markers to identify the extent of geothermal water activity [56]. The correlation between the minor components B, F, Li, and  $Cl^-$  suggests that geothermal water is mixed with deep fluid and that the formation of geothermal water is closely linked to deep magmatic activity in the geothermal field.

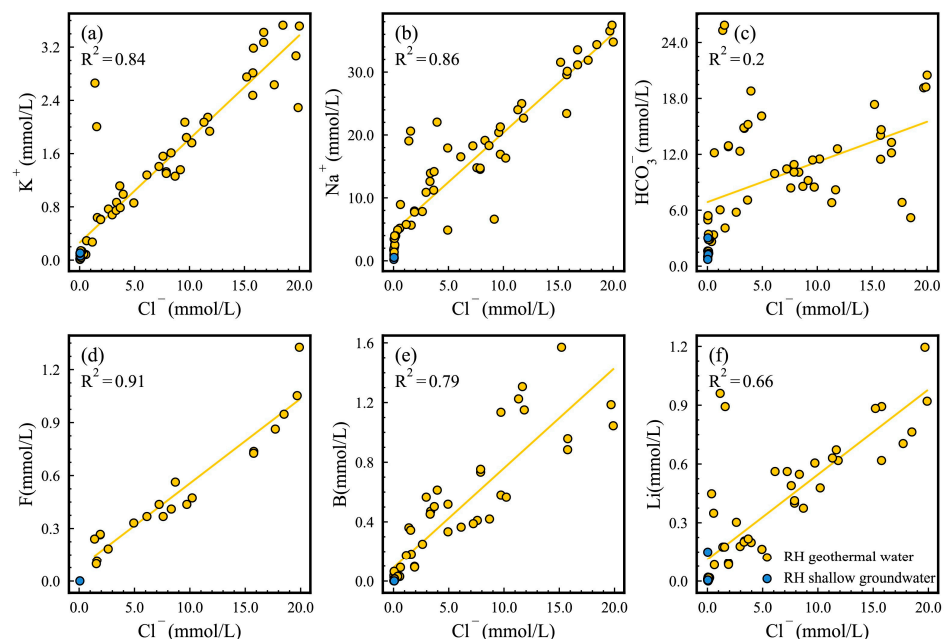


**Figure 16.** Correlation diagram of  $Cl^-$  and other hydration components of Rehai’s geothermal water. (a)  $K^+$  vs.  $Cl^-$  (b)  $Na^+$  vs.  $Cl^-$  (c)  $HCO_3^-$  vs.  $Cl^-$  (d) F vs.  $Cl^-$  (e) B vs.  $Cl^-$  (f) Li vs.  $Cl^-$ .

#### 4.3.4. Analysis of Water–Rock Equilibrium State

Most of the Rehai geothermal springs are located in partially equilibrated and immature water areas (Figure 17). This suggests that the water–rock reaction has not yet reached equilibrium [46]. The majority of the water samples collected originate from the shallow section of the geothermal system and are expected to mix with cold water during the ascent. Currently, the water–rock interaction is in its initial–intermediate stage [74]. Some geothermal springs are located on the equilibrium line, indicating that some of the water samples in the geothermal field originate from a relatively closed deep geothermal reservoir with a high temperature of up to 280 °C. This suggests that they are less affected by the mixing of shallow cold water. The Rehai geothermal water has not yet reached a state of full equilibrium, and the cationic geothermometers are, therefore, not applicable in the area.

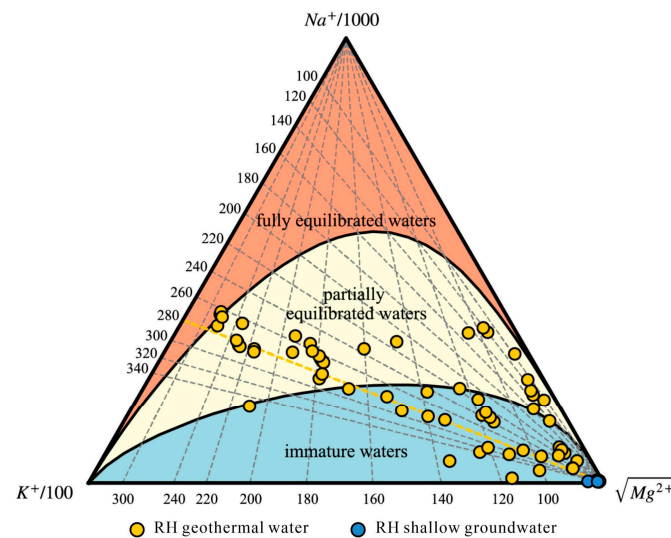


**Figure 17.** The Na–K–Mg triangle diagram [70] of Rehai's geothermal water.

#### 4.3.5. Reservoir Temperature

Quartz geothermometers estimate the temperature of the Rehai reservoir to be 81–282 °C, with an average of 174 °C. The temperature of the Rehai geothermal reservoir is estimated by chalcedony geothermometers to be 49–282 °C, with an average of 154 °C (Table S1). Given that the estimated mean values of the two estimation methods exceed 150 °C, the estimated mean value of the quartz geothermometer (174 °C) is taken as the lower limit of the Rehai geothermal reservoir's temperature. The maximum estimated temperature of the quartz and chalcedony geothermometers is consistent, indicating the calculation results are reliable. It is proposed that the geothermal reservoir temperature of the Rehai geothermal field is between 174 and 282 °C. This result is similar to that reported by Li et al. [77].

#### 4.4. Comparative Analysis of Yangbajing, Gudui, and Rehai Geothermal Fields

Differences exist in the geothermal reservoir environment of geothermal fluids of varying evolution types. As a result, the interaction of geothermal fluids with environmental media leads to the formation of distinct hydrochemical characteristics, element composition, and distribution patterns [74].

When comparing the Schoeller and Piper diagrams of the geothermal water in the three regions, it is evident that the hydrochemical types of the geothermal waters in the Yangbajing and Gudui geothermal fields are relatively simple, with the Cl–Na type being dominant. The Rehai geothermal field is characterised by geothermal springs that are primarily of the HCO<sub>3</sub>–Cl–Na type. The geothermal springs in Rehai originate from deep geothermal fluid (Cl–Na type water) that rises to a certain depth and is then contaminated by meteoric water and interacts with surrounding rocks before rising to the surface along

secondary fractures [30]. It is suggested that the underground hot water in Yangbajing and Gudui belongs to deep circulation, and the geological environment is relatively closed. The exchange capacity with the outside world is weak, the renewal rate is slow, and the water–rock interaction is strong [34,62]. However, the geological environment of the geothermal water in the Rehai geothermal system is relatively open. Its residence time is relatively short, and the water–rock interaction is still in its early stages [74].

The stable hydrogen and oxygen isotopes of the Yangbajing and Gudui geothermal fields are highly depleted, with  $\delta D$  and  $\delta^{18}O$  values much lower than those of the Rehai geothermal field. This is because the Yangbajing and Gudui geothermal fields are located in the southern part of the Qinghai–Tibet Plateau, with sampling elevations ranging from 4280 m to 4561 m and 4424 m to 4678 m, respectively. In contrast, the Rehai geothermal water is sampled at an elevation of 1417 m to 1946 m. The  $\delta D$  and  $\delta^{18}O$  values in meteoric water decrease with increasing altitude [60]. The primary recharge source for geothermal water in Yangbajing and Gudui is snow-melt water, while the Rehai geothermal field is mainly recharged by meteoric water. The calculation results indicate that all three geothermal fields have deep geothermal fluid sources. Rehai and Gudui geothermal fields have a high mixing ratio of magmatic water (subduction-related volcanic water), with averages of 22% and 21%, respectively. The mixing ratio of magmatic water in the Yangbajing geothermal field is relatively small, at 17%. The estimated results are basically consistent with previous conclusions (Rehai: mostly hot spring water <10%, some deep borehole water can reach 54%; Gudui: 21–24%; Yangbajing: 15–23%) [19,34,40].

The  $Cl^-$  ratio diagram shows the content of minor elements, including F, B, and Li. The highest content is observed in the Yangbajing geothermal field, followed by the Gudui geothermal field. In contrast, the Rehai geothermal field has significantly lower trace element content. This finding further verifies that the geological environment of the Rehai geothermal system is more open. After mixing the deep fluid with geothermal water, shallow cold water may also be mixed during the migration process, leading to a significant reduction in trace element content.

By comparing the distribution of geothermal water samples from Yangbajing, Gudui, and Rehai in the Na–K–Mg triangle diagram, it is evident that most of the samples from the Yangbajing and Gudui geothermal fields are located near the partial equilibrium water area. Additionally, the geothermal water sample points are significantly distant from the distribution of cold water points, and a linear trend in the sample point distribution is apparent. The sample points for geothermal water in the Rehai geothermal field are located in close proximity to the sample points for cold water. The linear distribution trend of the sample points is not well-defined. The difference in distribution may be attributed to the more significant water–rock reaction between the geothermal waters of Yangbajing and Gudui and the surrounding rock during the migration process. Additionally, the Rehai geothermal water (cold water mixing ratio: 60–70%) is mixed with more shallow cold water than Yangbajing (cold water mixing ratio: 40–50%) and Gudui (cold water mixing ratio: 20–40%) during the exposure process [30,55,60].

The geothermal water in the study area is immature, partially balanced or mixed water, rendering it unsuitable for the use of cation geothermometers in calculating the geothermal reservoir temperature. The silica dissolved in natural water is generally not affected by other ions, nor by the formation and volatilisation of complexes, and the precipitation rate slows down with the decrease in temperature. Consequently, the concentration of silica in shallow groundwater can be employed to indicate the temperature of an underground geothermal reservoir. The quartz and chalcedony geothermometers can be utilised to calculate the temperature of thermal reservoirs [73]. Based on previous estimates, the Rehai geothermal field has the highest reservoir temperature at 282 °C, followed by Gudui at 266 °C, and Yangbajing at 237 °C. When comparing the average temperature of geothermal springs in the Rehai, Gudui, and Yangbajing fields (72 °C, 81 °C, and 77 °C, respectively), it is evident that the temperature of the geothermal springs does not necessarily increase with the temperature of the geothermal reservoir. The higher mixing ratio of cold water

and the more open geological environment in the Rehai geothermal field result in greater heat loss during the rising process of geothermal water [37,78].

## 5. Development and Utilization of Geothermal Resources

In summary, there are high-temperature geothermal reservoirs in the three geothermal fields of Yangbajing, Gudui, and Rehai which can meet the needs of geothermal power generation or geothermal heating. The systematic understanding and study of the genesis, occurrence state, and circulation process of these geothermal resources can provide a valuable theoretical basis for the exploitation and utilization of geothermal resources. However, at present, only in the Yangbajing geothermal field has work successfully been carried out on geothermal energy power generation, and the development and utilization of both the Gudui and the Rehai geothermal fields are weak. Therefore, subsequent research work on the development and utilization of geothermal resources needs to be strengthened. Work can be carried out such as (1) strengthening the construction of geothermal energy power generation. There are high-temperature geothermal springs and geothermal jets in the Gudui and Rehai areas, and geothermal steam power generation or geothermal water power generation units can be selected according to different types: geothermal steam power generation through the heat exchanger unit on the steam group decompression, expansion, purification for power generation; geothermal water power generation through the vacuum to obtain water vapour, and the use of low-boiling-point material steam to do work to generate electricity [79]. (2) Strengthening the development of physical therapy in hot springs. Hot spring water has good medical value, which can treat arthritis and reduce the probability of skin diseases. The development of hot-springs physiotherapy has low requirements for equipment, technology, and cost, and is the simplest and most direct way to develop and utilize geothermal resources. (3) Strengthening the construction of geothermal heating. The average annual temperature in Tibet is only 2.5 °C [19], and heating is vital to the lives of people in the Tibetan region. The equipment for geothermal heating is more complex compared to spa physiotherapy, and usually requires the use of a geothermal heat pump to extract hot water to a converter, which converts low-grade energy into high-grade energy for heating. (4) Strengthening the research and development of geothermal equipment and mining technology. At present, there are problems with the equipment and technology of the geothermal power station in Yangbajing, such as different degrees of scaling and corrosion occurring in the pipeline of the extracted geothermal water, so that the safety and stability of the thermal system of the power station and the thermal control system are reduced, and the operating costs are increased; the implementation of tail water recharge of geothermal water is not sufficient, which restricts the sustainable development of geothermal water [80,81]. For high-temperature geothermal resources, the binary flashing cycle system has been developed to add a flasher and a mass pump to simultaneously increase power generation capacity and ensure system stability [82].

In addition to the Yangbajing, Gudui, and Rehai geothermal fields studied in this paper, there are more than 200 high-temperature hydrothermal systems with reservoir temperatures higher than 150 °C distributed in the HBG, which have great potential for exploration and development [17]. Future work should focus on other potential high-temperature geothermal resources and conduct more extensive hydrogeological and geochemical investigations, including on hydrochemistry, isotopes, and gases. This will aid in understanding, improving, and evaluating the distribution, characteristics, and development potential of high-temperature geothermal resources in western China. It is of great significance to promote the development of clean geothermal energy in China.

## 6. Conclusions

1. The geothermal springs in the Yangbajing, Gudui, and Rehai geothermal fields are primarily sourced from deep Cl-Na geothermal fluids. The geological environments of the Yangbajing and Gudui geothermal fields are relatively closed, resulting in a low proportion of cold water mixing. The hydrochemical type of the exposed

- geothermal springs is predominantly Cl-Na. The Rehai geothermal field has an open geological environment with a high proportion of shallow cold water. This causes the hydrochemical type of the geothermal spring to change from a Cl-Na type to an HCO<sub>3</sub>-Cl-Na type due to water–rock interaction and mixing with shallow cold water.
2. The geothermal waters in Yangbajing and Gudui are primarily recharged by snow-meltwater and magmatic water, with magmatic water accounting for 17% and 21%, respectively. The geothermal waters are mainly recharged by local meteoric water and subduction-related volcanic water (with an average mixing ratio of 22%). The recharge elevations of the three geothermal fields are 5174–5736 m, 4764–5186 m, and 1182–2350 m, respectively.
  3. The Rehai geothermal field boasts the highest thermal reservoir temperature at 282 °C, followed by the Gudui geothermal field at 266 °C, and finally the Yangbajing geothermal field at 237 °C. Due to significant heat loss during the rising process in the Rehai geothermal field, the average temperature of the exposed geothermal springs in this area is lower than that of the Yangbajing and Gudui areas.

**Supplementary Materials:** The following supporting information can be downloaded at: <https://www.mdpi.com/article/10.3390/w16101378/s1>, Table S1: Hydrochemical and physical compositions of geothermal and cold waters in the Yangbajing, Gudui and Rehai geothermal fields; Table S2:  $\delta D$  and  $\delta^{18}O$  compositions of geothermal and cold waters in the Yangbajing, Gudui and Rehai geothermal field. References [83–89] are cited in Supplementary Materials.

**Author Contributions:** Conceptualization, Q.L. and X.Y.; methodology, Q.L.; software, Y.H.; validation, X.Y.; formal analysis, C.L.; investigation, Q.L.; resources, J.H.; data curation, J.H.; writing—original draft preparation, Q.L.; writing—review and editing, X.Y.; visualization, J.H.; supervision, C.L.; project administration, Y.H.; funding acquisition, X.Y. All authors have read and agreed to the published version of the manuscript.

**Funding:** This research was funded by The Scientific Key R&D project of the Tibet Autonomous Region, grant number [XZ202201ZY0021G], the National Natural Science Foundation of China, grant number [42072313, 42102334], the Sichuan Provincial Department of Science and Technology Projects, grant number [2022NSFSC0413, 2023YFS0356], the Yibin Government Foundation, grant number [SWJTU2021020007, SWJTU2021020008].

**Data Availability Statement:** Research data have been listed within the manuscript.

**Conflicts of Interest:** Authors Q.L. and Y.H. were employed by the China Railway Construction Kunlun Investment Group Company Limited. The remaining authors declare that the research was conducted in the absence of any commercial or financial relationships that could be construed as a potential conflict of interest.

## References

1. Lund, J.W.; Toth, A.N. Direct utilization of geothermal energy 2020 worldwide review. *Geothermics* **2021**, *90*, 101915. [[CrossRef](#)]
2. Wang, Y.; Yuan, X.; Zhang, Y.; Zhang, X.; Xiao, Y.; Duo, J.; Huang, X.; Sun, M.; Lv, G. Hydrochemical, D–O–Sr isotopic and electromagnetic characteristics of geothermal waters from the Erdaoqiao area, SW China: Insights into genetic mechanism and scaling potential. *Ore Geol. Rev.* **2023**, *158*, 105486. [[CrossRef](#)]
3. Zhou, H.; Kuang, X.; Hao, Y.; Wang, C.; Feng, Y.; Zou, Y.; Zhu, M.; Zheng, C. Magmatic fluid input controlling the geochemical and isotopic characteristics of geothermal waters along the Yadong-Gulu rift, southern Tibetan Plateau. *J. Hydrol.* **2023**, *619*, 129196. [[CrossRef](#)]
4. National Energy Administration. 13th Five-Year Plan for Modern Energy System. Available online: [https://www.nea.gov.cn/135989417\\_14846217874961n.pdf](https://www.nea.gov.cn/135989417_14846217874961n.pdf) (accessed on 14 March 2024). (In Chinese)
5. Wang, G.L.; Zhang, W.; Liang, J.Y.; Lin, W.; Liu, Z.M.; Wang, W. Evaluation of Geothermal Resources Potential in China. *Acta Geosci. Sin.* **2017**, *38*, 449–459. [[CrossRef](#)]
6. He, P.; Zhang, H.; Li, S.; Zhou, X.; Zhou, X.; He, M.; Tian, J.; Zhang, Y.; Wu, Z.; Chen, T.; et al. Geological and hydrochemical controls on water chemistry and stable isotopes of hot springs in the Three Parallel Rivers Region, southeast Tibetan Plateau: The genesis of geothermal waters. *Sci. Total Environ.* **2023**, *906*, 167648. [[CrossRef](#)]
7. Muffler, P.; Cataldi, R. Methods for regional assessment of geothermal resources. *Geothermics* **1978**, *7*, 53–89. [[CrossRef](#)]
8. Guo, Q.; Pang, Z.; Wang, Y.; Tian, J. Fluid geochemistry and geothermometry applications of the Kangding high-temperature geothermal system in eastern Himalayas. *Appl. Geochem.* **2017**, *81*, 63–75. [[CrossRef](#)]

9. Arellano, V.M.; Garcia-Gutierrez, A.; Barragan, R.M.; Izquierdo, G.; Nieva, D. An updated conceptual model of the Los Humeros geothermal reservoir (Mexico). *J. Volcanol. Geotherm. Res.* **2003**, *124*, 67–88. [[CrossRef](#)]
10. Sanada, T.; Takamatsu, N.; Yoshiike, Y. Geochemical interpretation of long-term variations in rare earth element concentrations in acidic hot spring waters from the Tamagawa geothermal area, Japan. *Geothermics* **2006**, *35*, 141–155. [[CrossRef](#)]
11. Taussi, M.; Nisi, B.; Brogi, A.; Liotta, D.; Zucchi, M.; Venturi, S.; Cabassi, J.; Boschi, G.; Ciliberti, M.; Vaselli, O. Deep Regional Fluid Pathways in an Extensional Setting: The Role of Transfer Zones in the Hot and Cold Degassing Areas of the Larderello Geothermal System (Northern Apennines, Italy). *Geochem. Geophys. Geosyst.* **2023**, *24*, e2022GC010838. [[CrossRef](#)]
12. Taussi, M.; Brogi, A.; Liotta, D.; Nisi, B.; Perrini, M.; Vaselli, O.; Zambrano, M.; Zucchi, M. CO<sub>2</sub> and heat energy transport by enhanced fracture permeability in the Monterotondo Marittimo-Sasso Pisano transfer fault system (Larderello Geothermal Field, Italy). *Geothermics* **2022**, *105*, 102531. [[CrossRef](#)]
13. Tian, J.; Pang, Z.; Guo, Q.; Wang, Y.; Li, J.; Huang, T.; Kong, Y. Geochemistry of geothermal fluids with implications on the sources of water and heat recharge to the Rekeng high-temperature geothermal system in the Eastern Himalayan Syntax. *Geothermics* **2018**, *74*, 92–105. [[CrossRef](#)]
14. Christenson, B.W.; Mroczek, E.K.; Kennedy, B.M.; Soest, M.C.V.; Stewart, M.K.; Lyon, G. Ohaaki reservoir chemistry: Characteristics of an arc-type hydrothermal system in the Taupo Volcanic Zone, New Zealand. *J. Volcanol. Geotherm. Res.* **2002**, *115*, 53–82. [[CrossRef](#)]
15. Karaku, H. Helium and carbon isotope composition of gas discharges in the Simav Geothermal Field, Turkey: Implications for the heat source. *Geothermics* **2015**, *57*, 213–223. [[CrossRef](#)]
16. Gola, G.; Bertini, G.; Bonini, M.; Botteghi, S.; Brogi, A.; De Franco, R.; Dini, A.; Donato, A.; Gianelli, G.; Liotta, D.; et al. Data integration and conceptual modelling of the Larderello geothermal area, Italy. *Energy Procedia* **2017**, *125*, 300–309. [[CrossRef](#)]
17. Guo, Q. Hydrogeochemistry of high-temperature geothermal systems in China: A review. *Appl. Geochem.* **2012**, *27*, 1887–1898. [[CrossRef](#)]
18. Wu, Y.; Zhou, X. Structural control effects on hot springs' hydrochemistry in the northern Red River Fault Zone: Implications for geothermal systems in fault zones. *J. Hydrol.* **2023**, *623*, 129836. [[CrossRef](#)]
19. Yang, H.; Yuan, X.; Chen, Y.; Liu, J.; Zhan, C.; Lv, G.; Hu, J.; Sun, M.; Zhang, Y. Geochemical Evidence Constraining Genesis and Mineral Scaling of the Yangbajing Geothermal Field, Southwestern China. *Water* **2023**, *16*, 24. [[CrossRef](#)]
20. Naik, P.K.; Awasthi, A.K.; Mohan, P.C. Springs in a headwater basin in the Deccan Trap country of the Western Ghats, India. *Hydrogeol. J.* **2002**, *10*, 553–565. [[CrossRef](#)]
21. Lv, G.; Zhang, X.; Wei, D.; Yu, Z.; Yuan, X.; Sun, M.; Kong, X.; Zhang, Y. Water–Rock Interactions, Genesis Mechanism, and Mineral Scaling of Geothermal Waters in Northwestern Sichuan, SW China. *Water* **2023**, *15*, 3730. [[CrossRef](#)]
22. Tian, J.; Stefánsson, A.; Li, Y.; Li, L.; Xing, L.; Li, Z.; Li, Y.; Zhou, X. Geochemistry of thermal fluids and the genesis of granite-hosted Huangshadong geothermal system, Southeast China. *Geothermics* **2023**, *109*, 102647. [[CrossRef](#)]
23. Zhang, Y.; Xu, M.; Li, X.; Qi, J.; Zhang, Q.; Guo, J.; Yu, L.; Zhao, R. Hydrochemical Characteristics and Multivariate Statistical Analysis of Natural Water System: A Case Study in Kangding County, Southwestern China. *Water* **2018**, *10*, 80. [[CrossRef](#)]
24. Guo, Q.; Planer-Friedrich, B.; Liu, M.; Yan, K.; Wu, G. Magmatic fluid input explaining the geochemical anomaly of very high arsenic in some southern Tibetan geothermal waters. *Chem. Geol.* **2019**, *513*, 32–43. [[CrossRef](#)]
25. Li, X.; Qi, J.; Yi, L.; Xu, M.; Zhang, X.; Zhang, Q.; Tang, Y. Hydrochemical characteristics and evolution of geothermal waters in the eastern Himalayan syntaxis geothermal field, southern Tibet. *Geothermics* **2021**, *97*, 102233. [[CrossRef](#)]
26. Singh, H.K.; Chandrasekharan, D.; Raju, N.J.; Ranjan, S. Geothermal energy potential in relation to black carbon reduction and CO<sub>2</sub> mitigation of Himalayan geothermal belt—A review. *Geothermics* **2024**, *119*, 102962. [[CrossRef](#)]
27. Zhang, C.; Shi, Q.; Lingjuan, Z. Discussion on the relationship between Cenozoic magmatic activity and geotherm in Tibetan Plateau. *Geol. Surv. China* **2018**, *5*, 18–24. [[CrossRef](#)]
28. Liao, Z.; Zhao, P. *Yunnan–Tibet Geothermal Belt—Geothermal Resources and Case Histories*; Science Press: Beijing, China, 1999.
29. Duo, J. The basic characteristics of the Yangbajing geothermal field—A typical high temperature geothermal system. *Eng. Sci.* **2003**, *5*, 42–47.
30. Wang, S. Hydrogeochemical Processes and Genesis Mechanism of High-temperature Geothermal System in Gudui, Tibet. Ph.D. Thesis, China University of Geosciences, Beijing, China, 2017. (In Chinese).
31. Ma, R.; Shi, J.; Liu, J.; Gui, C. Combined use of multivariate statistical analysis and hydrochemical analysis for groundwater quality evolution: A case study in north chain plain. *J. Earth Sci.* **2014**, *25*, 587–597. [[CrossRef](#)]
32. Zhang, Y. *Study on the Genesis and Development and Utilization of Geothermal System in Kangding-Moxi Section of Xianshuihe Fault*; Chengdu University of Technology: Chengdu, China, 2018.
33. Hou, Z.; Mo, X.; Gao, Y.; Yang, Z.; Dong, G.; Ding, L. Early Processes and Tectonic Model for the Indian-Asian Continental Collision: Evidence from the Cenozoic Gangdese Igneous Rocks in Tibet. *Acta Geol. Sin.* **2006**, *80*, 1233–1248.
34. Wang, C.; Zheng, M.; Zhang, X.; Xing, E.; Zhang, J.; Ren, J.; Ling, Y. O, H, and Sr isotope evidence for origin and mixing processes of the Gudui geothermal system, Himalayas, China. *Geosci. Front.* **2020**, *11*, 1175–1187. [[CrossRef](#)]
35. Elenga, H.I.; Tan, H.; Su, J.; Yang, J. Origin of the enrichment of B and alkali metal elements in the geothermal water in the Tibetan Plateau: Evidence from B and Sr isotopes. *Geochemistry* **2021**, *81*, 125797. [[CrossRef](#)]
36. Wang, S. Distribution of Conjugate Angles of Seismic Faults in the Qinghai-Tibet Plateau and Its Implications for Continental Dynamics. *Acta Geol. Sin.* **2004**, *78*, 475–481.

37. Wang, P.; Chen, X.; Shen, L.; Xiao, Q.; Wu, X. Reservoir temperature of geothermal anomaly area and its environmental effect in Tibet. *Geol. China* **2016**, *43*, 1429–1438. [[CrossRef](#)]
38. Wang, Y.; Li, L.; Wen, H.; Hao, Y. Geochemical evidence for the nonexistence of supercritical geothermal fluids at the Yangbajing geothermal field, southern Tibet. *J. Hydrol.* **2022**, *604*, 127243. [[CrossRef](#)]
39. Meng, H.R.; Cao, R.; Chen, D.F.; Ngawang, G.; Luo, W.X.; Cai, Y.Q.; Yan, Y.M. Types, Distribution Characteristics, and Exploration Direction of Hydrothermal Alteration in Gudui Geothermal Field, Tibet. *Acta Geosci. Sin.* **2023**, *44*, 158–168. [[CrossRef](#)]
40. Yuan, J.; Cao, H.; Guo, Y.; Chen, X. Source and Evolution of Subduction-Related Hot Springs Discharged in Tengchong Geothermal Field, Southwest China: Constrained by Stable H, O, and Mg Isotopes. *Minerals* **2022**, *12*, 1490. [[CrossRef](#)]
41. Zhang, M.; Guo, Z.; Sano, Y.; Zhang, L.; Sun, Y.; Cheng, Z.; Yang, T.F. Magma-derived CO<sub>2</sub> emissions in the Tengchong volcanic field, SE Tibet: Implications for deep carbon cycle at intra-continent subduction zone. *J. Asian Earth Sci.* **2016**, *127*, 76–90. [[CrossRef](#)]
42. Guo, Q.; Wang, Y.; Liu, W. Major hydrogeochemical processes in the two reservoirs of the Yangbajing geothermal field, Tibet, China. *J. Volcanol. Geotherm. Res.* **2007**, *166*, 255–268. [[CrossRef](#)]
43. Wang, C.; Zheng, M. Hydrochemical Characteristics and Evolution of Hot Fluids in the Gudui Geothermal Field in Comei County, Himalayas. *Geothermics* **2019**, *81*, 243–258. [[CrossRef](#)]
44. Liu, M. Source of Hydrochemical Composition and Formation Mechanism of Rehai Geothermal Water in Tengchong. *Safety and Environmental Engineering*. **2014**, *21*, 1–7. (In Chinese) [[CrossRef](#)]
45. Shanguan, Z.; Sun, M.; Li, H. Active types of modern geothermal fluids at the Tengchong region, Yunnan province. *Seismol. Geol.* **1999**, *21*, 437–442.
46. Guo, Q.; Wang, Y. Geochemistry of hot springs in the Tengchong hydrothermal areas, Southwestern China. *J. Volcanol. Geotherm. Res.* **2012**, *215–216*, 61–73. [[CrossRef](#)]
47. Li, J.; Sagoe, G.; Yang, G.; Liu, D.; Li, Y. The application of geochemistry to bicarbonate thermal springs with high reservoir temperature: A case study of the Batang geothermal field, western Sichuan Province, China. *J. Volcanol. Geotherm. Res.* **2019**, *371*, 20–31. [[CrossRef](#)]
48. Brown, L.D.; Zhao, W.; Nelson, K.D.; Hauck, M.; Alsdorf, D.; Ross, A.; Cogan, M.; Clark, M.; Liu, X.; Che, J. Bright Spots, Structure, and Magmatism in Southern Tibet from INDEPTH Seismic Reflection Profiling. *Science* **1996**, *274*, 1688–1690. [[CrossRef](#)] [[PubMed](#)]
49. Nelson, K.D.; Zhao, W.; Brown, L.D.; Kuo, J.; Che, J.; Liu, X.; Klemperer, S.L.; Makovsky, Y.; Meissner, R.; Mechie, J.; et al. Partially Molten Middle Crust Beneath Southern Tibet: Synthesis of Project INDEPTH Results. *Science* **1996**, *274*, 1684–1688. [[CrossRef](#)] [[PubMed](#)]
50. Chen, L.; Booker, J.R.; Jones, A.G.; Wu, N.; Unsworth, M.J.; Wei, W.; Tan, H. Electrically Conductive Crust in Southern Tibet from INDEPTH Magnetotelluric Surveying. *Science* **1996**, *274*, 1694–1696. [[CrossRef](#)] [[PubMed](#)]
51. Kind, R.; Ni, J.; Zhao, W.; Wu, J.; Yuan, X.; Zhao, L.; Sandvol, E.; Reese, C.; Nabelek, J.; Hearn, T. Evidence from Earthquake Data for a Partially Molten Crustal Layer in Southern Tibet. *Science* **1996**, *274*, 1692–1694. [[CrossRef](#)] [[PubMed](#)]
52. Tan, H.; Wei, W.; Martyn, U.; Deng, M.; Jin, S. Crustal electrical conductivity structure beneath the Yarlung Zangbo Jiang suture in the southern Xizang plateau. *Chin. J. Geophys.* **2004**, *47*, 685–690.
53. Bai, D.; Liao, Z.; Zhao, G.; Wang, X. The Inference of Magmatic Heat Source Beneath the Rehai (Hot Sea) Field of Tengchong From the Result of Magnetotelluric Sounding. *Chin. Sci. Bull.* **1994**, *39*, 572–577.
54. Fang, N. Study on Geological Characteristics and Formation Mechanism of Tengchong Rehai Geothermal Field. Master's Thesis, Kunming University of Science and Technology, Kunming, China, 2013. (In Chinese)
55. Guo, T. Study on the Characteristics and Genesis of Rehai Geothermal Field in Tengchong, Yunnan. Ph.D. Thesis, Kunming University of Science and Technology, Kunming, China, 2013. (In Chinese)
56. Sun, M. *Hydrochemical Characteristics and Genetic Mechanism of Geothermal Resource in the Yangbajing Area, Tibet*; Tibet University: Lhasa, China, 2023. (In Chinese)
57. Duoji. Typical high temperature geothermal system-basic characteristics of Yangbajing geothermal field. *Strateg. Study CAE* **2003**, *5*, 42–47. (In Chinese)
58. Zhao, C.; Ran, H.; Chen, K. Present-day magma chambers in Tengchong volcano area inferred relative geothermal gradient. *Acta Petrol. Sin.* **2006**, *22*, 1517–1528.
59. Wang, G. *Geothermal Resources in China*; Sciences Press: Beijing, China, 2018. (In Chinese)
60. Guo, Q.; Wang, Y.; Liu, W. O, H, and Sr isotope evidences of mixing processes in two geothermal fluid reservoirs at Yangbajing, Tibet, China. *Environ. Earth Sci.* **2010**, *59*, 1589–1597. [[CrossRef](#)]
61. Pang, Z. pH dependant isotope variations in arc-type geothermal waters: New insights into their origins. *J. Geochem. Explor.* **2006**, *89*, 306–308. [[CrossRef](#)]
62. Sun, H.; Ma, F.; Lin, W.; Liu, Z.; Wang, G.; Nan, D. Geochemical Characteristics and Geothermometer Application in High Temperature Geothermal Field in Tibet. *Geol. Sci. Technol. Inf.* **2015**, *34*, 171. (In Chinese)
63. Zhao, P.; Jin, J.; Zhang, H.; Ji, D.; Liang, T. Chemical composition of thermal water in the Yangbajing geothermal field, Tibet. *Chin. J. Geol.* **1998**, *33*, 61–72.
64. Piper, A. A Graphic Procedure in the Geochemical Interpretation of Water-Analyses. *Eos Trans. Am. Geophys. Union* **1944**, *25*, 914–923.
65. Craig, H. Isotopic variations in meteoric waters. *Science* **1961**, *133*, 1702–1703. [[CrossRef](#)] [[PubMed](#)]

66. Yu, J.; Zhang, H.; Yu, F.; Liu, D. Oxygen and hydrogen isotopic compositions of meteoric waters in the eastern part of Xizang. *Chin. J. Geochem.* **1984**, *13*, 93–101. [[CrossRef](#)]
67. Arnórsson, S.; Andrésdóttir, A. Processes controlling the distribution of boron and chlorine in natural waters in Iceland. *Geochim. Et Cosmochim. Acta* **1995**, *59*, 4125–4146. [[CrossRef](#)]
68. Truesdell, A.H.; Nathenson, M.; Rye, R.O. The effects of subsurface boiling and dilution on the isotopic compositions of Yellowstone thermal waters. *J. Geophys. Res.* **1977**, *82*, 3694–3704. [[CrossRef](#)]
69. Tassi, F.; Aguilera, F.; Darrah, T.; Vaselli, O.; Capaccioni, B.; Poreda, R.J.; Delgado Huertas, A. Fluid geochemistry of hydrothermal systems in the Arica-Parinacota, Tarapacá and Antofagasta regions (northern Chile). *J. Volcanol. Geotherm. Res.* **2010**, *192*, 1–15. [[CrossRef](#)]
70. Giggenbach, W.F. Geothermal solute equilibria. derivation of Na-K-Mg-Ca geothermometers. *Geochim. Et Cosmochim. Acta* **1988**, *52*, 2749–2765. [[CrossRef](#)]
71. Henley, R.W.; Ellis, A.J. Geothermal systems ancient and modern: A geochemical review. *Earth-Sci. Rev.* **1983**, *19*, 1–50. [[CrossRef](#)]
72. Tan, H.; Zhang, Y.; Zhang, W.; Kong, N.; Zhang, Q.; Huang, J. Understanding the circulation of geothermal waters in the Tibetan Plateau using oxygen and hydrogen stable isotopes. *Appl. Geochem.* **2014**, *51*, 23–32. [[CrossRef](#)]
73. Zhang, W.; Wang, G.; Zhao, J.; Liu, F. Geochemical Characteristics of Medium-high Temperature Geothermal Fluids in West Sichuan and Their Geological Implications. *Geoscience* **2021**, *35*, 188–198. [[CrossRef](#)]
74. Ma, Z. A comparative study of isotopic hydrogeochemistry of geothermal fluids of sedimentary basin type and volcanic type. *Hydrogeol. Eng. Geol.* **2019**, *46*, 9–18. [[CrossRef](#)]
75. Fan, Y.; Chen, Y.; Li, X.; Li, W.; Li, Q. Characteristics of water isotopes and ice-snowmelt quantification in the Tizinafu River, north Kunlun Mountains, Central Asia. *Quat. Int.* **2015**, *380–381*, 116–122. [[CrossRef](#)]
76. Long, M. Characteristics and Formation of Some of the Hot Springs in Tengchong County of Yunnan. Master's Thesis, China University of Geosciences, Beijing, China, 2015. (In Chinese)
77. Li, J.; Guo, Q.; Wang, Y. Evaluation of temperature of parent geothermal fluid and its cooling processes during ascent to surface: A case study in Rehai geothermal field, Tengchong. *Earth Sci.* **2015**, *40*, 1576–1584. [[CrossRef](#)]
78. Li, Z. Modern Geothermal Water Activities during the Collisional Orogeny of the Qinghai-Tibet Plateau. Ph.D. Thesis, Chinese Academy of Geological Sciences, Beijing, China, 2002. (In Chinese)
79. Zhao, X.; Fu, H. Analysis of current status and prospects of geothermal energy development and utilization. *Environ. Dev.* **2019**, *31*, 233–235.
80. Li, Y.; Pang, Z.; Galeczka, I.M. Quantitative assessment of calcite scaling of a high temperature geothermal well in the Kangding geothermal field of Eastern Himalayan Syntax. *Geothermics* **2020**, *87*, 101844. [[CrossRef](#)]
81. Zhao, B.; Lyu, Y.; Wen, R.; Gong, Y.; Wang, S. Utilization situation and development prospect of geothermal energy in Tibet. *Therm. Power Gener.* **2023**, *52*, 1–6.
82. Wang, L.; Li, H.; Bu, X. Multi-objective optimization of Binary Flashing Cycle (BFC) driven by geothermal energy. *Appl. Therm. Eng.* **2020**, *166*, 114693. [[CrossRef](#)]
83. Fournier, R.O.; Potter, R.W., II. A Revised and expanded silica (quartz) geothermometer. *Bull. Geoth. Resour. Counc.* **1982**, *11*, 3–12.
84. Can, İ. A new improved Na/K geothermometer by artificial neural networks. *Geothermics* **2002**, *31*, 751–760. [[CrossRef](#)]
85. Fournier, R.O.; Truesdell, A.H. An empirical NaKCa geothermometer for natural waters. *Geochim. Cosmochim. Acta* **1973**, *37*, 1255–1275. [[CrossRef](#)]
86. Zhang, W.; Tan, H.; Zhang, Y.; Wei, H.; Dong, T. Boron geochemistry from some typical Tibetan hydrothermal systems: Origin and isotopic fractionation. *Appl. Geochem.* **2015**, *63*, 436–445. [[CrossRef](#)]
87. Yan, K.; Wan, D. Study on chemical characteristics and formation mechanism of Tengchong Rehai hot spring group. *J. Seismol. Res.* **1998**, *21*, 9. (In Chinese)
88. Yuan, J. Transport of Boron in the Aquatic Environment of the Yangbajing Geothermal Field, Tibet. Master's Thesis, China University of Geosciences (Wuhan), Wuhan, China, 2010.
89. Zhou, L. Characteristics of Typical Hot SPRINGS in central Tibet. Master's Thesis, China University of Geosciences (Beijing), Beijing, China, 2012. (In Chinese)

**Disclaimer/Publisher's Note:** The statements, opinions and data contained in all publications are solely those of the individual author(s) and contributor(s) and not of MDPI and/or the editor(s). MDPI and/or the editor(s) disclaim responsibility for any injury to people or property resulting from any ideas, methods, instructions or products referred to in the content.